

# Interacting spin droplets and magnetic properties of a low-density two-dimensional electron gas

Yevgeny V. Stadnik and Oleg P. Sushkov

*School of Physics, University of New South Wales, Sydney 2052, Australia*

(Received 27 December 2012; revised manuscript received 15 August 2013; published 3 September 2013)

We argue that the magnetic susceptibility data for the low-density two-dimensional (2D) silicon-based electron gas indicate that magnetically active electrons are localized in spin droplets. The droplets exist in both the insulating and metallic phases, and interact ferromagnetically, forming an effective 2D Heisenberg ferromagnet. Comparing the data with analytical and numerical results for a 2D Heisenberg ferromagnet, we determine parameters of the model and show that the value of the droplet spin is either  $S = 1/2$  or  $S = 1$  with very few electrons in the droplet. We discuss the dependence of the magnetic susceptibility and the specific heat on the external magnetic field, which follows from the model, and hence we suggest further experimental tests of the model.

DOI: [10.1103/PhysRevB.88.125402](https://doi.org/10.1103/PhysRevB.88.125402)

PACS number(s): 71.30.+h, 75.25.-j, 75.75.-c

## I. INTRODUCTION

Studies of low density two-dimensional electron gas (2DEG) systems attract great attention, because of the unusual and rich properties of these systems. In the present work, we consider the magnetic properties of a silicon based 2DEG discovered in recent studies.<sup>1–3</sup> Most likely the properties are related to the metal-insulator phase transition (MIT), and, in our opinion, understanding of these properties sheds some light on the nature of the transition.

The MIT in a 2DEG has attracted protracted attention from both experiment and theory, and remains a puzzling area of research to date.<sup>4–20</sup> It was once believed that a MIT in such systems could not take place, because a true metallic phase does not exist in a noninteracting 2DEG,<sup>8</sup> although extension of the scaling theory of localization to include the effects of interaction<sup>9,10</sup> suggested that a MIT may be possible. Resistivity measurements in a silicon-based 2DEG finally provided evidence for a true MIT,<sup>12</sup> with numerous works following thereafter and studying the transition.<sup>13–24</sup> The mechanism for a MIT in a 2DEG remains unclear to this date, but the existence of localized states on the insulator side of a MIT is generally accepted.<sup>5,6,25–27</sup>

Intimately linked to the problem of the MIT is the nature of the ground state of a 2DEG, which still remains an outstanding problem.<sup>20,22–24</sup> The ground state depends on electron density. There is little doubt that at a sufficiently high density it is a normal paramagnetic Fermi liquid.<sup>28</sup> At a lower density, the system might have a Stoner transition to a ferromagnetic Fermi liquid,<sup>29</sup> and ultimately at a very low density it must undergo a transition to the Wigner crystal.<sup>30</sup> These are scenarios for a 2DEG without any extrinsic disorder; see Refs. 31–34. Extrinsic disorder can further complicate the situation; see, for instance, Refs. 35 and 36.

The magnetization and magnetic susceptibility of a silicon based 2DEG in the electron density range below and above a MIT have been studied recently.<sup>1–3,23</sup> The experiments have been performed with an in-plane magnetic field and so only spin related magnetic properties have been measured. There are three important outcomes of these measurements. (i) Thermodynamic magnetic properties vary continuously across the MIT. (ii) The zero-field magnetic susceptibility diverges rapidly in the limit  $T \rightarrow 0$ ,  $\chi_0 \propto 1/T^{2.4}$ , in both

the insulating and metallic phases. (iii) In the metallic phase at  $T \sim \text{few K}$ , the value of the susceptibility is by orders of magnitude larger than the expected value of the ideal gas Pauli susceptibility.

The authors of Refs. 1–3 explain their data through the formation of electron droplets. Each droplet has a nonzero spin. These droplets melt in the metallic phase with increasing density and temperature, but continue to exist up to large densities. At a fixed density of droplets, this picture would give the usual Curie scaling of the susceptibility with temperature,  $\propto 1/T$ . To explain the observed scaling,  $\propto 1/T^{2.4}$ , Ref. 3 suggests that the density of droplets is decreasing when temperature is increasing.

In the present work, we take a somewhat different view to explain the magnetic data. We agree that the data practically unambiguously indicate the formation of electron droplets with nonzero spin. The droplets are probably formed due to extrinsic disorder or extrinsic disorder assisted by the Coulomb interaction. Pragmatically for our purposes, the exact mechanism of their formation is not important. We only assume that at low temperatures all the internal degrees of freedom of the droplets are frozen and hence the only dynamical degree of freedom is the spin of the droplet. The very steep temperature dependence of the magnetic susceptibility, in our opinion, indicates ferromagnetic instability.

There has been an early analysis of magnetic susceptibility data for 2DEG.<sup>37</sup> The analysis was based on the model of random *antiferromagnetic* interactions between localized spins. A random antiferromagnetic interaction always results in a spin glass state with magnetic susceptibility diverging at  $T \rightarrow 0$  slower than the Curie's law,  $\chi \propto 1/T^\alpha$ ,  $\alpha < 1$ . This is true for both classical<sup>38,39</sup> and quantum<sup>40</sup> spins. On the other hand the data<sup>1–3</sup> unambiguously indicate much stronger divergence than the Curie's law. The only possible, in theory, example with stronger divergence is the 2D quantum ferromagnet which, according to the Mermin-Wagner theorem,<sup>41</sup> has zero Curie temperature. Therefore we conjecture a random ferromagnetic interaction between droplets and hence consider the system as a quantum ferromagnetic Heisenberg model. On theoretical side the ferromagnetic Heisenberg model is simpler than the antiferromagnetic one. A random antiferromagnetic model is always magnetically frustrated and this results in a complex spin-glass state qualitatively different from the ground state

of the nonrandom antiferromagnetic Heisenberg model.<sup>38–40</sup> A random ferromagnetic model is unfrustrated and this results in simple ferromagnetic ground state identical to that of the nonrandom ferromagnetic Heisenberg model. The randomness (disorder) is irrelevant.

Thus, the data indicate the ferromagnetic Heisenberg model for the insulating phase and we also assume that the localized droplets described by the Heisenberg model continue to exist in the metallic phase. While in the metallic phase most electrons go into itinerant states, these electrons are magnetically almost idle and the main contribution to the magnetic susceptibility is due to the relatively small fraction of electrons localized in the droplets. The density of the droplets diminishes in the metallic phase with increasing electron density.

We will show that there are only few electrons in the droplet (maybe even one electron) and therefore the term “droplet” is not quite suitable. Nevertheless, we use the term following Refs. 1–3.

The structure of the paper is as follow. Section II reviews known properties of the 2D quantum Heisenberg ferromagnet at very low temperatures and we also derive some previously unknown properties, which we need for the present work. In Sec. III we analyze the high-temperature series expansions for magnetic susceptibility and check that the intermediate-high-temperature and the low-temperature descriptions are consistent in the overlapping region. We also discuss here the universality of series expansions. Comparison with experimental data is performed in Sec. IV. This allows us to determine parameters of the droplets and their exchange interactions. In Sec. V, we make predictions, which can be checked experimentally. Finally, Sec. VI presents our conclusions.

## II. 2D QUANTUM HEISENBERG FERROMAGNET AT VERY LOW TEMPERATURES

The Heisenberg model is defined by the Hamiltonian

$$H_J = -J \sum_{(ij)} \mathbf{S}_i \cdot \mathbf{S}_j. \quad (1)$$

In this section for simplicity we assume that the model is defined on a square lattice. Summation in (1) is performed over nearest sites and  $\mathbf{S}_i$  is the quantum spin at the site  $i$ . In the ground state, all spins are aligned ferromagnetically along, say, the  $z$  axis. Excitations are spin waves with the following spectrum:<sup>42</sup>

$$\varepsilon_{\mathbf{k}} = 2JS[2 - \cos(k_x) - \cos(k_y)] \xrightarrow{k \ll 1} JSk^2. \quad (2)$$

Hereafter we set the Planck constant and the Boltzmann constant equal to unity,  $\hbar = k_B = 1$ .

Each spin-wave excitation carries spin  $\Delta S_z = -1$ . The excitations are bosons and therefore the magnetization at a nonzero temperature is

$$\langle S_z \rangle = S - \int \frac{1}{e^{\varepsilon_{\mathbf{k}}/T} - 1} \frac{d^2k}{(2\pi)^2}. \quad (3)$$

The integral is logarithmically diverging at small momenta. This is a direct consequence of the Mermin-Wagner theorem,<sup>41</sup> which claims that a long-range order is impossible in a 2D system at a nonzero temperature. The ferromagnetic ordering

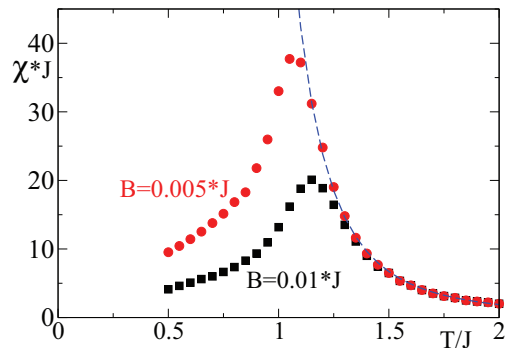


FIG. 1. (Color online) Magnetic susceptibility per site obtained in QMC simulations of  $S = 1$  Heisenberg model (Ref. 45). Values of the magnetic field are  $B = 0.005J$  (red circles) and  $B = 0.01J$  (black squares). The blue dashed line shows the simple exponential fit (10).

exists only within a correlation length  $\xi$ . To find value of  $\xi$ , one has to set  $\langle S_z \rangle = 0$  and impose a lower limit in the integration in (3),  $k > k_{\min} \sim 1/\xi$ . This gives the following correlation length in the low-temperature limit:<sup>43</sup>

$$\xi \propto e^{2\pi JS^2/T}. \quad (4)$$

There are  $\mathcal{N} \sim \xi^2$  spins within the correlation length; these spins act as a magnetic domain with total magnetic moment  $M \sim S\mathcal{N}$ . The concentration of domains is  $n_D \sim 1/\mathcal{N}$ . All in all, this describes a superparamagnet with the following magnetic susceptibility,  $\chi \propto n_D M^2 \propto \mathcal{N} \propto \xi^2 \propto e^{4\pi JS^2/T}$ . This simple logic does not give the prefactor before the exponential. The renormalization group (RG) calculation gives<sup>44</sup>

$$\chi_{RG} = A \frac{S}{T} \left( \frac{T}{4\pi JS^2} \right)^3 e^{4\pi JS^2/T}, \quad (5)$$

where  $A$  is a constant. Note that the third power of the semiclassical parameter  $\frac{T}{4\pi JS^2}$  in the prefactor in (5) arises in the two-loop approximation, while the single loop approximation gives only the first power of the parameter.

Quantum Monte Carlo (QMC) simulation of the magnetic susceptibility for  $S = 1/2$  was performed in Ref. 44 and for  $S = 1$  in Ref. 45. In this section we refer to the results of Ref. 45, because this simulation accounts for a nonzero magnetic field. The susceptibility QMC data<sup>45</sup> for the values of magnetic field  $B = 0.005J$  and  $B = 0.01J$  are presented in Fig. 1.

Interaction with uniform magnetic field is defined by the Hamiltonian

$$H_B = H_J - B \sum_i S_{iz}. \quad (6)$$

Even a very small magnetic field significantly influences the susceptibility at very low temperature. Equation (5) is valid only at  $T \ll JS$ , but on the other hand, due to the presence of a magnetic field, the temperature cannot be too low,  $T > T_m$ . Here  $T_m$  is the temperature where the susceptibility is maximum; see Fig. 1. The value of  $T_m$  depends on the magnetic field. The very strong dependence of the susceptibility on the magnetic field is related to the dimensionality of the system.

To explain the dependence, we remind that at zero temperature the magnon dispersion in a magnetic field at small  $k$  is<sup>42</sup>

$$\varepsilon_{\mathbf{k}} = JSk^2 + B. \quad (7)$$

When deriving Eqs. (4) and (5), we substitute in (3)  $k_{\min} \sim 1/\xi$  as the lower limit of integration. This is correct only if  $JS/\xi^2 > B$ . From this condition, one immediately finds  $T_m$

$$T_m \sim \frac{4\pi JS^2}{\ln\left(\frac{4\pi JS^2}{B}\right)}. \quad (8)$$

The dependence on the magnetic field is logarithmic and hence even a tiny magnetic field significantly influences the susceptibility. The estimate (8) is valid only at asymptotically small magnetic field. At higher fields one needs to use numerics. According to Ref. 45 at  $B/J = 0.1$  the value of  $T_m$  is  $T_m \approx 0.5J$  at  $S = 1/2$  and  $T_m \approx 1.6J$  at  $S = 1$ . As soon as temperature is slightly larger than  $T_m$ ,  $T > 1.1T_m$  the susceptibility becomes independent of  $B$ . This is clearly seen in Fig. 1 where data for different values of magnetic field are significantly different for  $T < T_m$  and are practically identical for  $T > 1.1T_m$ .

The RG expression (5) for magnetic susceptibility is valid at low temperature,  $T \ll JS$ , as it follows from the dispersion (2). On the other hand, the temperature must be higher than  $T_m$ . So the region of validity of Eq. (5) is

$$T_m \ll T \ll JS. \quad (9)$$

This shows that the magnetic field and hence the temperature in the QMC data in Fig. 1 is not sufficiently small to compare the data at  $T > T_m$  with RG formula (5). The data are nicely fitted by the simple exponential formula

$$\chi = 0.042e^{7.6J/T}. \quad (10)$$

The fit is shown in Fig. 1 by the blue dashed line. Since the condition (9) is not fulfilled the exponent in (10) is different from that predicted by RG, Eq. (5).

Formula (10) is valid in a rather narrow range of temperatures; at  $T \gg J$  the formula gives the susceptibility approaching a constant instead of expected Curie's law,

$\chi = S(S+1)/(3T)$ . The transition region between the exponential behavior and the asymptotic Curie's law is described by expansion in series of  $J/T$ . This is exactly where the experimental data<sup>1-3</sup> are taken. We discuss the series expansions in Sec. III.

The low temperature ( $T \ll JS$ ) and zero magnetic field specific heat per lattice site immediately follows from the dispersion (2),

$$C = \frac{T}{2\pi JS} \int_0^\infty \frac{x dx}{e^x - 1} = \frac{\pi}{12} \frac{T}{JS}. \quad (11)$$

Interestingly, the temperature dependence of the specific heat is the same as that for a 2D Fermi gas,  $C_F = \frac{\pi^2}{3} \frac{T}{\epsilon_F}$ , however, the behavior in an external magnetic field is distinctly different from that of a gas. The specific heat of the ferromagnet is suppressed in the field  $B \sim T$ , while the specific heat of the Fermi gas is not very sensitive to the field.

### III. 2D QUANTUM HEISENBERG FERROMAGNET AT INTERMEDIATE TEMPERATURES: SERIES EXPANSIONS

The fifth-order temperature series for ferromagnetic Heisenberg model (1) and (6) have been derived in Ref. 46 for square and triangular lattices. We are not aware of higher-order calculations; the fifth order is sufficient for our purposes. The expansion is in powers of the parameter

$$x = \frac{ZS(S+1)J}{3T}, \quad (12)$$

where  $Z$  is the number of nearest neighbors (the coordination number). The magnetic susceptibility reads

$$\chi = \frac{S(S+1)}{3T} F \quad (13)$$

$$F = 1 + b_1x + b_2x^2 + b_3x^3 + b_4x^4 + b_5x^5 + \dots$$

Explicit analytic expressions for the coefficients  $b_i$  are very long. They are presented in the original paper.<sup>46</sup> To illustrate convergence we present below the series for  $S = 1/2$  and  $S = 1$ .

$$S = 1/2 : \begin{cases} \text{Square lattice: } & F = 1 + x + 0.5x^2 + 0.167x^3 + 0.068x^4 + 0.037x^5 + \dots \\ \text{Triangular lattice: } & F = 1 + x + 0.667x^2 + 0.315x^3 + 0.116x^4 + 0.045x^5 + \dots \end{cases} \quad (14)$$

$$S = 1 : \begin{cases} \text{Square lattice: } & F = 1 + x + 0.656x^2 + 0.375x^3 + 0.188x^4 + 0.087x^5 + \dots \\ \text{Triangular lattice: } & F = 1 + x + 0.771x^2 + 0.500x^3 + 0.288x^4 + 0.154x^5 + \dots \end{cases}$$

A comparison of the series expansion (14) for  $S = 1$  square lattice with quantum Monte Carlo simulations<sup>45</sup> (the same QMC data as in Fig. 1) is shown in Fig. 2.

Note that here we compare theory with theory, just different asymptotic representation of the same susceptibility. From comparison of series with QMC we conclude that the used series expansion for  $S = 1$  is satisfactory at  $T/J > 1.6$ , i.e., at  $x < 1.65$ . So, the value  $x = 1.65$  is the maximum value of  $x$  where we can rely on the series. At this limit the accuracy of series is about several percent. For  $S = 1/2$  the maximum

value of  $x$ , assuming the same accuracy, is about  $x = 1.9$ . At higher temperatures (smaller  $x$ ) the series are very accurate. In the same Fig. 2 we plot the exponential fit of QMC data (10). The fit obviously does not give the right high-temperature behavior.

Let us check how the type of lattice and value of spin influence the function  $F(x)$ . Since the system is not frustrated, *a priori* we expect an almost universal behavior. The function  $F$  is plotted in the top panel of Fig. 3 for square and for triangular lattice Heisenberg models for spins  $S = 1/2, 1, 2$ .

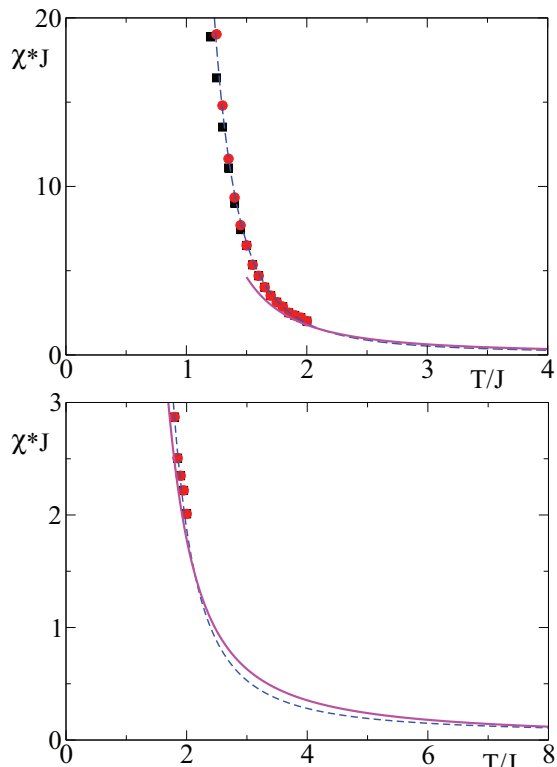


FIG. 2. (Color online) Magnetic susceptibility per site for  $S = 1$  square lattice Heisenberg model. Results of QMC simulations (Ref. 45) are shown by symbols. Values of the magnetic field are  $B = 0.005J$  (red circles) and  $B = 0.01J$  (black squares). The magenta solid line shows the series result (14). The dashed blue line shows the exponential fit (10) of QMC data. The top and the bottom panels show the same plot in different scales.

The plots confirm that the dependence of  $F$  on the type of lattice and on the spin is very weak. Moreover, having in mind that we will use  $F$  to fit experimental data with unknown values of  $S$ ,  $Z$ , and  $J$  we always can rescale the variable  $x$ ,  $x \rightarrow \alpha x$ . The plots of  $F(\alpha x)$  vs  $1/x$  are shown in the bottom panel of Fig. 3. We chose the square lattice with  $S = 1$  as the reference lattice, so here  $\alpha = 1$ . For other situations the rescaling factors are as follows: square lattice with  $S = 1/2$ ,  $\alpha = 1.21$ ; square lattice with  $S = 2$ ,  $\alpha = 0.93$ ; triangular lattice with  $S = 1$ ,  $\alpha = 0.91$ . With the rescaling the curves for  $F$  collapse to the almost universal function shown in the bottom panel.

#### IV. COMPARISON WITH EXPERIMENTAL MAGNETIC SUSCEPTIBILITY DATA

Experimental susceptibility data<sup>1</sup> are presented in Fig. 4. The MIT occurs at  $n = n_{\text{MIT}} = 0.85$ , hereafter for densities we use units  $10^{11} \text{ cm}^{-2}$ . The data at densities close to MIT,  $n = 0.55, 0.88, 1.43$ , we call the “upper set of data” and the data deep inside the metallic phase,  $n = 4.3$ , we call the “lower set of data”; see Fig. 4. To fit the data we use the high-temperature Heisenberg model expansion

$$\chi/n(\mu_B/T) = A \frac{T_0}{T} \frac{F(x)}{F(x_0)}, \quad (15)$$

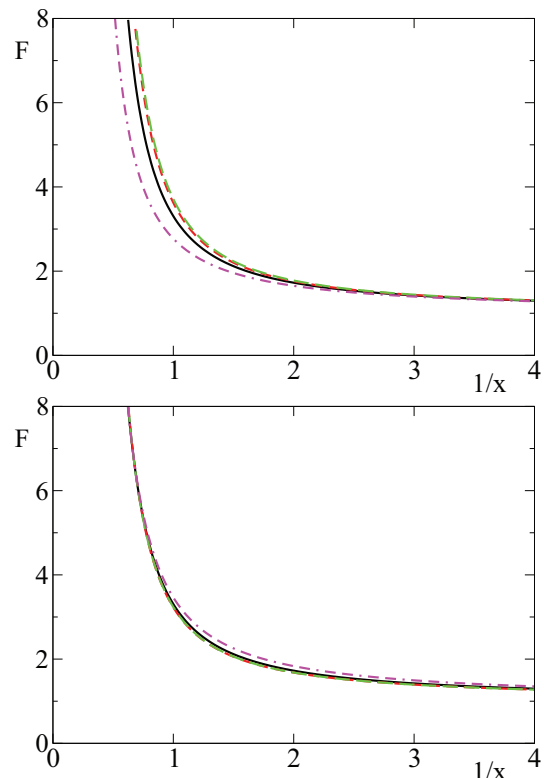


FIG. 3. (Color online) Top panel: Function  $F(x)$  vs  $1/x$  for four different Heisenberg models. Square lattice:  $S = 1/2$  (double-dashed-dotted magenta line),  $S = 1$  (black solid line), and  $S = 2$  (red dashed line). Triangular lattice  $S = 1$  (green long-dashed line). Bottom panel: Function  $F(\alpha x)$  vs  $1/x$  for the same models. The scaling factor  $\alpha$  is chosen to collapse all the curves to an almost universal function.

where  $T_0 = 1.7 \text{ K}$  is the minimum temperature where the data are available; Fig. 4. We already pointed out that  $F(x)$  is a practically universal function which is almost insensitive to spin and type of lattice. Changing spin/coordination number

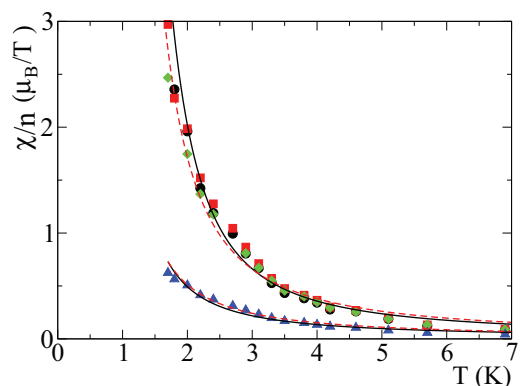


FIG. 4. (Color online) Experimental data (Ref. 1) for  $\chi/n$  vs temperature for various values of electron density  $n$ . Below values of  $n$  are given in units  $10^{11} \text{ cm}^{-2}$ . Black circles correspond to  $n = 0.55$ , red squares correspond to  $n = 0.88$ , green diamonds correspond to  $n = 1.43$ , and blue triangles correspond to  $n = 4.3$ . Solid black lines show the  $S = 1$  square lattice Heisenberg model fit and the dashed red lines show the  $S = 1/2$  square lattice Heisenberg model fit.



is equivalent to rescaling the variable  $x$ , i.e., rescaling the exchange integral  $J$ . To demonstrate this again we fit the data with square lattice. In Fig. 4 black solid lines correspond to  $S = 1$  and red dashed lines correspond to  $S = 1/2$ . The fitting parameters are

$$\begin{aligned} \text{upper set: } & S = 1, \quad J = 1.05 \text{ K}, \quad A = 3.5 \\ & S = 1/2, \quad J = 3 \text{ K}, \quad A = 2.76; \\ \text{lower set: } & S = 1, \quad J = 0.7 \text{ K}, \quad A = 0.73 \\ & S = 1/2, \quad J = 2 \text{ K}, \quad A = 0.73. \end{aligned} \quad (16)$$

The maximum value of  $x$  with these parameters and with  $T > 1.7 \text{ K}$  is within the region of validity of series expansions discussed in Sec. III. The fits presented in Fig. 4 are quite good. We reiterate again that the fits are not sensitive to a particular lattice geometry and spin. For example, we can assume triangular lattice with spin  $S = 1$ . The fitting curves practically coincide with the black solid lines presented in Fig. 4, however the exchange integral is different, for example for the upper set of data  $J' = 0.93 \frac{4}{6} J \approx 0.65 \text{ K}$ . The robustness of the behavior/fits is due to the unfrustrated character of ferromagnetic interaction. So, fits of the temperature dependence of magnetic susceptibility confirm validity of the Heisenberg model and reliably determine the following combination of parameters:

$$\begin{aligned} \text{upper set of data: } & ZS(S+1)J \approx 9 \text{ K}; \\ \text{lower set of data: } & ZS(S+1)J \approx 6 \text{ K}. \end{aligned} \quad (17)$$

Since we deal with random droplets (random lattice) the meaning of  $ZS(S+1)J$  is

$$ZS(S+1)J \rightarrow S(S+1) \sum_{nn} J_i, \quad (18)$$

where  $nn$  denotes nearest neighbors and the right-hand side certainly assumes averaging over droplets.

In the insulating phase,  $n < n_{MIT}$ , all electrons are localized, so the total electron density  $n$  is equal to the density of localized electrons  $n_l$ . It is natural to assume that in the metallic phase,  $n > n_{MIT}$ , the density of localized electrons is roughly independent of  $n$  and is equal to  $n_l \approx n_{MIT}$ . With account of this argument, the  $n = 4.3$  data (the lower set) have to be scaled up by a factor of  $n/n_{MIT} = 4.3/0.85 \sim 5$ . After this scaling, the ‘‘lower set’’ is getting closer to the ‘‘upper set.’’

In the insulating phase,  $n < n_{MIT}$ , the separation between droplets is increasing when the electron density is decreasing,  $l \propto 1/\sqrt{n}$ . The ferromagnetic exchange  $J$  has the usual Hund-like origin and hence it depends exponentially on the separation,  $J \propto \exp(-l/R)$ , where  $R$  is the radius of localization (radius of the droplet). At MIT  $R \sim l$  and this corresponds to the density  $n = 0.85$ . The minimum density with available data is  $n = 0.55$ . So compared to MIT  $l$  is changed by factor  $\sqrt{0.85/0.55} \approx 1.25$ . The variation is too small to have a sizable effect on  $J$  and this is why we do not see the variation in the data. To see a sizable effect one needs to go to a significantly smaller density. We also discuss this issue in Sec. V.

To estimate the spin of the droplet  $S$  and the number of electrons in the droplet  $N$  we need to analyze the absolute value of the magnetic susceptibility. We do this only in the insulating phase where all electrons are localized (the upper set

of data). The number density of droplets is  $n/N$ . Equation (13) gives the dimensionless theoretical magnetic susceptibility per droplet. Restoring Bohr magneton and Boltzmann constant we rewrite (13) in terms of surface susceptibility,  $\chi/(n/N) = \frac{S(S+1)(g\mu_B)^2}{3k_B T} F(x)$ . We will assume that the spin  $g$  factor is  $g = 2$ . Equation (15) fits the experimental susceptibility per electron,  $\chi/n$ , presented in Fig. 4. The experimental value is given in Bohr magnetons per one T per electron. Equating the theoretical expression with fit of data,

$$\begin{aligned} \frac{\chi}{n} &= \frac{4}{3} \frac{S(S+1)}{N} \frac{\mu_B^2}{k_B T} F(x) \\ &\rightarrow \frac{4}{3} \frac{S(S+1)}{N} \frac{\mu_B B_0}{k_B T} F(x) = A \frac{T_0}{T} \frac{F(x)}{F(x_0)}, \end{aligned} \quad (19)$$

we get the following relation:

$$\frac{S(S+1)}{N} = \frac{3}{4} \frac{k_B T_0}{\mu_B B_0} \frac{A}{F(x_0)}. \quad (20)$$

Here  $B_0 = 1 \text{ T}$ . The fitting parameters are given in Eq. (16). From both  $S = 1$  [ $x_0 = 1.65$ ,  $F(x_0) = 8.58$ ] and  $S = 1/2$  [ $x_0 = 1.76$ ,  $F(x_0) = 6.50$ ] upper set fits we get

$$\frac{S(S+1)}{N} \approx 0.77. \quad (21)$$

This is the value of the ratio determined from the measured susceptibility.

The set  $S = 1/2$ ,  $N = 1$  perfectly fits the measured ratio. Another possibility is  $S = 1$ ,  $N = 4$  which gives  $S(S+1)/N = 0.5$ . According to Ref. 47 the  $N = 4$  droplet can have spin 1. One cannot exclude a possibility of  $S = 1/2$ ,  $N = 3$  droplet. In this case  $S(S+1)/N = 0.25$ , but in the end the ratio is determined from the prefactor and uncertainty about factor 2–3 is probably possible. Higher values of  $S$  and  $N$  seem unlikely; one needs extremely fine tuning with higher  $S$  and  $N$ . Thus, we conclude that the combinations  $S = 1/2$ ,  $N = 1$ ;  $S = 1$ ,  $N = 4$ ; and  $S = 1/2$ ,  $N = 3$  are the most likely. We know that the experimental saturation spin magnetization in the insulating phase is roughly  $\sim 50\%$  of the maximum possible spin magnetization.<sup>1,23</sup> This is approximately consistent with all the combinations which we have pointed out above.

A small droplet with  $N = 1$  or  $N = 3$  electrons naturally has spin  $S = 1/2$ . For  $N = 4$  the value of spin can be either  $S = 0$  or  $S = 1$  ( $S = 2$  is practically impossible). Many-body calculations for small 2D quantum dots<sup>47</sup> show that the ground-state spin of a four-electron dot is  $S = 1$ , already at a rather moderate value of Coulomb repulsion. Note that in referring to this we imply that the two-valley dispersion degeneracy in 2D silicon is not relevant; the valley hybridization is sufficiently large, at least 3–4 K. Due to the hybridization, electrons occupy only the bonding combination of valleys and the droplet is similar to the  $N = 4$  quantum dot in GaAs.<sup>47</sup> Without such hybridization, the spin of the  $N = 4$  quantum dot in silicon would be  $S = 0$ , because two electrons with total spin  $S = 0$  would occupy one valley and the other two electrons also with  $S = 0$  would occupy another valley.

At the lowest measured density,  $n \sim 0.5$ , the linear dependence of magnetization on magnetic field is observed at  $g\mu_B B \lesssim 0.1 \text{ K}$ ; see Fig. 1(c) in Ref. 3. The dependence is strongly nonlinear at higher fields. Comparing this value

with the low-density parameters in (16) (the ‘‘upper set’’) one concludes that the dimensionless magnetic field,  $g\mu_B B/J$ , in the linear regime is smaller than 0.1 in the case of  $S = 1$  and smaller than 0.03 in the  $S = 1/2$  case. Hence  $T_m < 1.6$  K for  $S = 1$  and  $T_m < 1.2$  K for  $S = 1/2$ ; see discussion in Sec. II. This proves that the analysis of data in Fig. 4 at  $T > 1.7$  K with field-independent susceptibility is self-consistent.

Concluding this section we summarize the main points. (i) The experimental data demonstrate a very singular behavior of the susceptibility as  $T \rightarrow 0$  in the insulating phase. The singularity is much stronger than the Curie one. In our opinion, this indicates a 2D quantum Heisenberg ferromagnet. This is our major observation. Very good fits of experimental data obtained using high-temperature series expansions confirm validity of this conjecture. (ii) The random Heisenberg ferromagnet is magnetically unfrustrated and this is why we can use the analysis results obtained for nonrandom Heisenberg ferromagnets. (iii) Since the system is unfrustrated the ground state is the usual ferromagnet; there is no spin-glass behavior. (iv) Usage of high-temperature series expansions in the analysis allows us to reliably determine the prefactor in the susceptibility and hence find the spin and the number of electrons in the droplet. The most likely combinations are  $S = 1/2$ ,  $N = 1, 3$  and  $S = 1$ ,  $N = 4$ .

## V. HOW TO FURTHER CHECK THE HEISENBERG MODEL PICTURE?

The low-temperature exponential divergence of the magnetic susceptibility in the 2D ferromagnetic Heisenberg model is necessarily accompanied by high sensitivity to the magnetic field. The dependence is clearly demonstrated in Fig. 1, where it manifests itself as  $T_m(B)$  with two distinct behaviors for  $T < T_m$  and  $T > T_m$ . Alternatively, one can consider the susceptibility (or magnetization) as a function of the magnetic field at a fixed temperature. This will also have two distinct regimes, one with approximately linear dependence of the magnetization on the magnetic field when  $B < B^*$  and one with very slow increase/saturation of magnetization at  $B > B^*$ . There are indications of such behavior in existing experimental data.<sup>1,2</sup> Further measurements and comparison with results of series expansions and Monte Carlo simulations can shed more light on this problem.

Another possibility to test the model is to measure the specific heat in a magnetic field in the insulating phase. We already pointed out in Sec. II that the magnetic field significantly and predictably modifies the specific heat. Again, a comparison with the results of series expansions and Monte Carlo simulations for the Heisenberg model would be very useful. An order of magnitude estimate of the effect immediately follows from Eq. (11) which gives the specific heat per site. Hence per unit area the specific heat is

$$C = \frac{\pi}{12} \frac{n_l}{N} \frac{T}{JS}. \quad (22)$$

We remind that  $n_l$  is density of localized electrons and  $N$  is the number of electrons per droplet. At  $T \sim J \sim 1$  K the specific heat is about  $\sim 0.1k_B$  per electron, where  $k_B$  is the Boltzmann constant. A magnetic field of about few T must suppress this specific heat to zero.

It is known that there are two mechanisms for interaction between localized spins: (i) the usual Hund-like exchange and (ii) superexchange.<sup>48</sup> The exchange mechanism leads to the ferromagnetic interaction, while superexchange leads to the antiferromagnetic one. We remind that we denote by  $R$  the radius of localization (radius of the droplet) and by  $l$  the separation between droplets. Obviously  $R < l$ . Usually at  $R \sim l$ , exchange wins and this, in our opinion, describes the present situation. On the other hand, at  $R \ll l \propto 1/\sqrt{n}$ , superexchange always wins,<sup>49</sup> leading to the random antiferromagnetic interaction. We already pointed out that a random antiferromagnetic interaction results in magnetic frustration and hence it results in a spin-glass state.<sup>38–40</sup> So, at a sufficiently low electron density below MIT we predict a density driven transition from the ferromagnetic state considered in the present work to a spin-glass state. Unfortunately we cannot quantitatively predict the critical density for the onset of the spin-glass state. Experimental indication for the transition (crossover) is a change in the temperature dependence of the magnetic susceptibility from the very singular,  $\propto \exp(\text{const}/T)$ , in the ferromagnetic state to a much less singular,  $\propto 1/T^\alpha$ ,  $\alpha < 1$ , in the spin-glass state.

## VI. CONCLUSIONS

We suggest the quantum Heisenberg ferromagnet model to explain the anomalous magnetic properties observed in the vicinity of the metal-insulator transition in a low-density two-dimensional silicon-based electron gas. The ferromagnet is composed of electron-spin droplets. The observed very steep temperature dependence of the magnetic susceptibility is associated with the intrinsic exponential divergence in the Heisenberg model. By comparing the experimental data with known analytical and numerical results for the 2D Heisenberg ferromagnet, we determine the parameters of the model,  $ZS(S+1)J \approx 9$  K, where  $Z$  is the effective coordination number,  $S$  is the spin of the droplet, and  $J$  is the ferromagnetic exchange constant between droplets. We further argue that most likely  $S = 1/2$  or  $S = 1$  with 1–4 electrons occupying each droplet on average. The 2D Heisenberg ferromagnet is strongly and distinctly influenced by magnetic field. Based on these properties, we suggest further experiments to test the model.

## ACKNOWLEDGMENTS

We are grateful to M. Reznikov, A. R. Hamilton, J. Oitmaa, and C. J. Hamer for important discussions. We thank N. Teneh for communicating experimental data.

<sup>1</sup>N. Teneh, A. Yu. Kuntsevich, V. M. Pudalov, T. M. Klapwijk, and M. Reznikov, arXiv:0910.5724.

<sup>2</sup>M. Reznikov, A. Y. Kuntsevich, N. Teneh, and V. M. Pudalov, *JETP Lett.* **92**, 470 (2010).

- <sup>3</sup>N. Teneh, A. Yu. Kuntsevich, V. M. Pudalov and M. Reznikov, *Phys. Rev. Lett.* **109**, 226403 (2012).
- <sup>4</sup>M. Imada, A. Fujimori, and Y. Tokura, *Rev. Mod. Phys.* **70**, 1039 (1998).
- <sup>5</sup>E. Abrahams, S. V. Kravchenko, and M. P. Sarachik, *Rev. Mod. Phys.* **73**, 251 (2001).
- <sup>6</sup>S. V. Kravchenko and M. P. Sarachik, *Rep. Prog. Phys.* **67**, 1 (2004).
- <sup>7</sup>V. Dobrosavljević, N. Trivedi and J. M. Valles, Jr., *Conductor-Insulator Quantum Phase Transitions*. (Oxford University Press, Oxford, 2012).
- <sup>8</sup>E. Abrahams, P. W. Anderson, D. C. Licciardello, and T. V. Ramakrishnan, *Phys. Rev. Lett.* **42**, 673 (1979).
- <sup>9</sup>A. M. Finkel'stein, *Sov. Phys. JETP* **57**, 97 (1983) [*Zh. Eksp. Teor. Fiz.* **84**, 168 (1983)].
- <sup>10</sup>A. M. Finkel'stein, *Sov. Phys. JETP* **59**, 212 (1983) [*Zh. Eksp. Teor. Fiz.* **86**, 367 (1983)].
- <sup>11</sup>A. Punnoose and A. M. Finkel'stein, *Science* **310**, 289 (2005).
- <sup>12</sup>S. V. Kravchenko, W. E. Mason, G. E. Bowker, J. E. Furneaux, V. M. Pudalov, and M. D'Iorio, *Phys. Rev. B* **51**, 7038 (1995).
- <sup>13</sup>V. Dobrosavljević, E. Abrahams, E. Miranda, and S. Chakravarty, *Phys. Rev. Lett.* **79**, 455 (1997).
- <sup>14</sup>D. Simonian, S. V. Kravchenko, and M. P. Sarachik, *Phys. Rev. B* **55**, R13421 (1997).
- <sup>15</sup>D. Simonian, S. V. Kravchenko, M. P. Sarachik, and V. M. Pudalov, *Phys. Rev. Lett.* **79**, 2304 (1997).
- <sup>16</sup>D. Popović, A. B. Fowler, and S. Washburn, *Phys. Rev. Lett.* **79**, 1543 (1997).
- <sup>17</sup>D. Simonian, S. V. Kravchenko, M. P. Sarachik, and V. M. Pudalov, *Phys. Rev. B* **57**, R9420 (1998).
- <sup>18</sup>J. S. Thakur and D. Neilson, *Phys. Rev. B* **59**, R5280 (1999).
- <sup>19</sup>S. A. Vitkalov, H. Zheng, K. M. Mertes, M. P. Sarachik, and T. M. Klapwijk, *Phys. Rev. Lett.* **87**, 086401 (2001).
- <sup>20</sup>A. A. Shashkin, S. V. Kravchenko, V. T. Dolgoplov, and T. M. Klapwijk, *Phys. Rev. Lett.* **87**, 086801 (2001).
- <sup>21</sup>V. M. Pudalov, M. E. Gershenson, H. Kojima, N. Butch, E. M. Dizhur, G. Brunthaler, A. Prinz, and G. Bauer, *Phys. Rev. Lett.* **88**, 196404 (2002).
- <sup>22</sup>E. Tutuc, S. Melinte, and M. Shayegan, *Phys. Rev. Lett.* **88**, 036805 (2002).
- <sup>23</sup>O. Prus, Y. Yaish, M. Reznikov, U. Sivan, and V. Pudalov, *Phys. Rev. B* **67**, 205407 (2003).
- <sup>24</sup>J. Zhu, H. L. Stormer, L. N. Pfeiffer, K. W. Baldwin, and K. W. West, *Phys. Rev. Lett.* **90**, 056805 (2003).
- <sup>25</sup>N. F. Mott, *Proc. Phys. Soc. London, Ser. A* **62**, 416 (1949).
- <sup>26</sup>P. W. Anderson, *Phys. Rev.* **109**, 1492 (1958).
- <sup>27</sup>A. R. Hamilton, M. Y. Simmons, M. Pepper, E. H. Linfield, and D. A. Ritchie, *Physica B* **296**, 21 (2001).
- <sup>28</sup>L. D. Landau, *Sov. Phys. JETP* **3**, 920 (1957); **5**, 101 (1957); **8**, 70 (1958).
- <sup>29</sup>E. C. Stoner, *Rep. Prog. Phys.* **11**, 43 (1947).
- <sup>30</sup>E. Wigner, *Phys. Rev.* **46**, 1002 (1934).
- <sup>31</sup>B. Tanatar and D. M. Ceperley, *Phys. Rev. B* **39**, 5005 (1989).
- <sup>32</sup>G. Senatore, S. Moroni, and D. Varsano, *Solid State Commun.* **119**, 333 (2001).
- <sup>33</sup>B. Bernu, L. Cândido, and D. M. Ceperley, *Phys. Rev. Lett.* **86**, 870 (2001).
- <sup>34</sup>C. Attaccalite, S. Moroni, P. Gori-Giorgi, and G. B. Bachelet, *Phys. Rev. Lett.* **88**, 256601 (2002).
- <sup>35</sup>K. Voelker and S. Chakravarty, *Phys. Rev. B* **64**, 235125 (2001).
- <sup>36</sup>G. Benenti, G. Caldara, and D. L. Shepelyansky, *Phys. Rev. Lett.* **86**, 5333 (2001).
- <sup>37</sup>A. Gold and V. T. Dolgoplov, *J. Phys.: Condens. Matter* **14**, 7091 (2002).
- <sup>38</sup>R. N. Bhatt and P. A. Lee, *J. Appl. Phys.* **52**, 1703 (1981).
- <sup>39</sup>R. N. Bhatt and P. A. Lee, *Phys. Rev. Lett.* **48**, 344 (1982).
- <sup>40</sup>J. Oitmaa and O. P. Sushkov, *Phys. Rev. Lett.* **87**, 167206 (2001).
- <sup>41</sup>N. D. Mermin and H. Wagner, *Phys. Rev. Lett.* **17**, 1133 (1966).
- <sup>42</sup>N. W. Ashcroft and N. D. Mermin, *Solid State Physics* (Harcourt College Publishers, Fort Worth, 1976).
- <sup>43</sup>M. Takahashi, *Phys. Rev. Lett.* **58**, 168 (1987).
- <sup>44</sup>P. Kopietz and S. Chakravarty, *Phys. Rev. B* **40**, 4858 (1989).
- <sup>45</sup>I. Juhasz Junger, D. Ihle, L. Bogacz, and W. Janke, *Phys. Rev. B* **77**, 174411 (2008).
- <sup>46</sup>N. V. Dalton, *Proc. Phys. Soc. (London)* **88**, 659 (1966).
- <sup>47</sup>C. Sloggett and O. P. Sushkov, *Phys. Rev. B* **71**, 235326 (2005).
- <sup>48</sup>More complex mechanisms for magnetic interaction are also known; see, e.g., A. A. Abrikosov, *Adv. Phys.* **29**, 869 (1980).
- <sup>49</sup>L. P. Gorkov and L. P. Pitaevskii, *Sov. Phys. Dokl.* **8**, 788 (1964); C. Herring and M. Flicker, *Phys. Rev.* **134**, A362 (1964).